5th ECPMG Delft · 2024

Proceedings of the 5th ECPMG 2024
5th European Conference on Physical Modelling in Geotechnics
2-4 October 2024, Delft, the Netherlands
© 2024 the Authors

A small-scale physical model for evaluating the axial response of Rock Anchors for offshore renewable applications

A. Genco
University of Dundee, Dundee, United Kingdom, 180026675@dundee.ac.uk

M. Ciantia, M. Previtali and M. Brown
University of Dundee, Dundee, United Kingdom, m.o.ciantia@dundee.ac.uk, m.previtali@dundee.ac.uk and m.j.z.brown@dundee.ac.uk

A. Ivanovic
University of Aberdeen, Aberdeen, United Kingdom, a.ivanovic@abdn.ac.uk

N. Cresswell and V. Twomey
SCHOTTEL Marine Technologies, Edinburgh, United Kingdom, nick.cresswell@schottel-mt.co.uk, and vincent.twomey@schottel-mt.co.uk

ABSTRACT: Rock Anchors (RAs) are a cost-effective solution to the expanding demand of renewable energy in the context of various deep-water applications. Novel anchoring systems designed for rocky seabeds require the development of simple installation procedures and reliable design methods under demanding loading conditions. In this work, a small-scale 1g physical test was developed to model the axial RA behaviour by means of pre-stressed anchor bolts installed in calcarenite rock. The load was applied through an UTM INSTRON machine, whilst a simple steel beam structure was adopted preventing vertical displacement of the calcarenite block. The failure mechanism and the load capacity under axial loading were experimentally assessed. The use of X-ray CT scans was found to be crucial in providing direct observations of installation effects and failure modes in the rock. The results presented in the paper can be used to validate the prediction of large-strain numerical models and develop rock-bolt interaction models to improve current design procedures.

1 INTRODUCTION

The increasing deployment of Offshore Renewable Energy (ORE) necessitates the development of innovative anchoring technologies to accommodate the expansion of offshore applications. To align with global climate objectives (IRENA-GWEC, 2022) the International Renewable Energy Agency (IRENA) underscores the ambitious target to produce 275 and 1,200 GW of ORE by 2030 and 2050, respectively. The Wind Europe 2022 report indicates 4% increase of wind power installation than last year in Europe, totalling 19 GW, of which offshore installations contributed 2.5 GW.

In the context of rocky seabed applications, Rock Anchors (RAs) emerge as a promising solution. The challenges lie in defining cost-efficient installation and reliable design methodologies minimizing the conservatism of traditional design practices, which predominantly rely on analytical and empirical methods, usually based upon assumptions on the rock failure geometry (Brown, 2015; Kim and Cho, 2012; Weerasinghe and Littlejohn, 1997). An advanced understanding of RA failure mechanisms through direct observations from field and physical tests can significantly enhance design procedures. Current experimental studies available in literature usually refer to classic grouted anchor bolts with a dearth information available for other technologies. This creates an emerging need for physical modelling to better explore and increase our understanding of the inception and propagation of RA failure mechanisms.

This paper presents 1g physical model testing of a novel RA design used for ORE. The host rock is a calcarenite already characterised in previous element testing campaigns (Ciantia and Di Prisco, 2016; Ciantia et al., 2015). RA installation and pullout are herein investigated by means of load displacement curves and by reporting potential damage effects using X-ray computed tomography at various stages of pullout. Displacement-controlled axial loading is applied using an UTM Instron testing device, while the vertical displacement of the rock block is prevented using a fixed steel beam in contact with its upper surface.

The results highlight the potential of small-scale 1g physical modelling to directly observe the failure mechanism of RAs in soft rocks. The pull-out failure mode observed is characterized by an initial phase

where local failure around the RA head can maintain the maximum load capacity. After large displacements this is followed by the formation of an almost axisymmetric wedge. These outcomes provide valuable insights for advancing RA design in ORE applications.

2 ROCK ANCHOR MODELLING

A novel rock anchoring technology designed to minimize the installation cost for ORE applications has been proposed by SCHOTTEL Marine Technologies (Figure 1). The RA proposed can be installed in various deep-water context where harsh marine conditions induce severe loading conditions. These loads will be transferred by the anchoring system and their magnitude will depend on the turbine size and mooring type (i.e. catenary, taut or semi-taut, and tension leg) (Randolph et al., 2011). Floating wind technologies typically harness a catenary mooring with a loading inclination which varies from 0 to 30° respects to the horizontal seabed plane (Cerfontaine et al., 2023) but could also be applied for taut moorings where loading is mainly vertical.

The RA is a groutless solution composed of an outer casing with expandable fingers at the bottom, a taper at the top end, and an inner stem with a lower sacrificial drill bit (Cresswell and Jeffcoate, 2016). Upon reaching the target depth, the inner system is retracted expanding the fingers and undercutting the rock, to secure the anchor in place. A nut is then tightenend applying pre-tension to the anchor, ensuring its stability in the seabed while minimising disturbance and reducing operational risk. The connection of the RA to the ORE platform is supported by means of pad-eye to interface with the mooring system, and its versatility allow for installation across various rock types and seabed conditions. The real size of the anchor has not been displayed for commercial reasons.

Figure 1. 3D visualisation of the groutless anchor designed by SCHOTTEL Marine Technologies.

The physical model analogue for the aforementioned anchor is represented through stainless sleeve anchor bolts for easy installation in soft rocks, a choice driven by the limitations of undercut anchor bolts, which are suitable only for hard rock or concrete, due to the higher interlocking and friction required for the installation (Béton, 1994). The sleeve anchor bolts used in this work transfer the load mainly by friction and are composed of a bolt, a conical wedge, and an outer expandable steel sleeve part (Figure 2b). Additionally, a washer and nut are used to fix the bolt at the top at the rock surface during the pre-tension phase. The main anchor bolt geometry properties are listed in Table 1 and represented in Figure 2. The steel used for the sleeve anchor has a Young's modulus $E_{steel} = 200\ MPa$. The anchor bolt has an embedment ratio (H/D) of 2.85 whilst the real anchor ratio is 9.00.

The installation procedure adopted for the physical test can be synthesized in the following steps: (i) drilling hole (Figure 2a), (ii) insertion of the sleeve anchor bolt (Figure 2b), and (iii) pre-tension of the anchor bolt (Figure 2c).

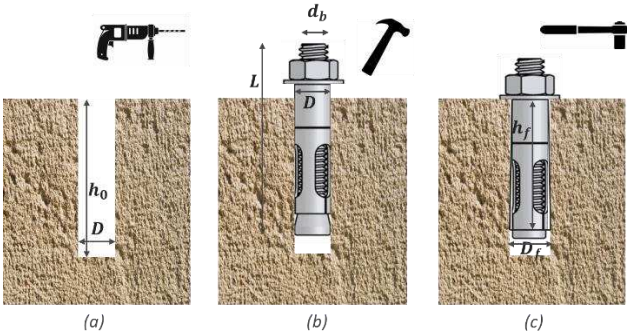

Figure 2. Sketch of the sleeve anchor bolt with geometric properties and installation procedure represented by: a) hole drilled, b) insertion, and c) pre-tension of the sleeve anchor bolt.

Table 1. The main sleeve anchor bolt properties

d_b [mm]	D [mm]	D_f [mm]	h_0 [mm]	h_f [mm]	L [mm]
8.0	14.0	17.0	60.0	40.0	87.0

A pillar drill was used to ensure axial drill alignment (Figure 2a) such that the diameter of the drilled hole is equal to the diameter of the sleeve part that encases the bolt. The potential presence of gap sensibly reduces the load capacity (Béton, 1994). Dust and debris in the drill hole were removed to ensure full contact between the rock and anchor and maximum capacity.

Upon drilling the hole, the sleeve anchor was inserted into the hole (Figure 2b). Specifically, at this configuration stage the cone wedge is located at the bottom part of the hole and the only forces acting on the system are the weight of the anchor and related reaction forces, as illustrated in Figure 3a.

The subsequent installation phase involves applying the pre-stress, executed through a torque wrench for the application of a specific torque moment

(Figure 2c). This action tightens the nut, driving the conical part upward, which in turn expands the sleeve part. This induces normal stresses at the rock-anchor interface crucial for the development of the frictional resistance (Figure 3b).

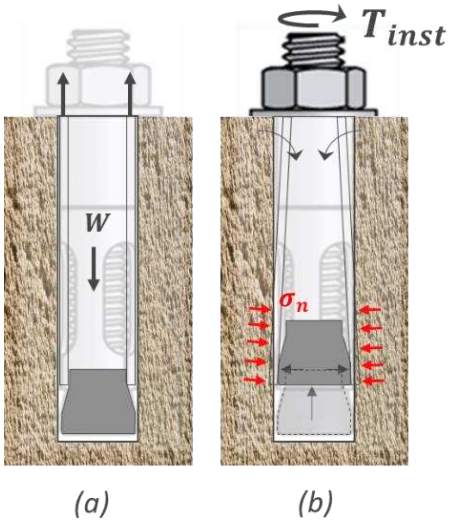

Figure 3. Detailed installation sketch which highlights the initial phase with the cone wedge in initial position (a) and subsequent phase (b) with the torque applied at the nut and related contact forces induced.

This installation process generates compressive stresses in the rock portion adjacent to the anchor base. The magnitude of the installation torque moment applied (T_{inst}) for the test performed is 15 Nm, following the specifications recommended in the anchor bolt technical documentation. Béton, (1994) states that a direct correlation appears between the pre-stress applied and the axial capacity of anchor bolts installed in concrete. This underscores the critical influence of pre-stressing on the overall capacity of anchor bolts, highlighting the role played by pre-tension on optimizing RA performance under axial loading.

2.1 Anchor installation effect in calcarenite

To advance the understanding of the rock-anchor interaction behaviour, this initial phase investigates installation and prestressing effects of sleeve anchor bolts in calcarenite rock. This rock type was chosen due to the wide availability of experimental data from literature. The calcarenite rock selected, belonging to the Calcarenite di Gravina (outcropping in Apulia, Southern Italy), is considered as soft rock which exhibits a brittle softening behaviour (Lollino and Andriani, 2017). Figure 4 shows the yield surface for the calcarenite used in this study while the main rock parameters are listed in Table 2. Further details on this rock are available from Ciantia et al., (2015).

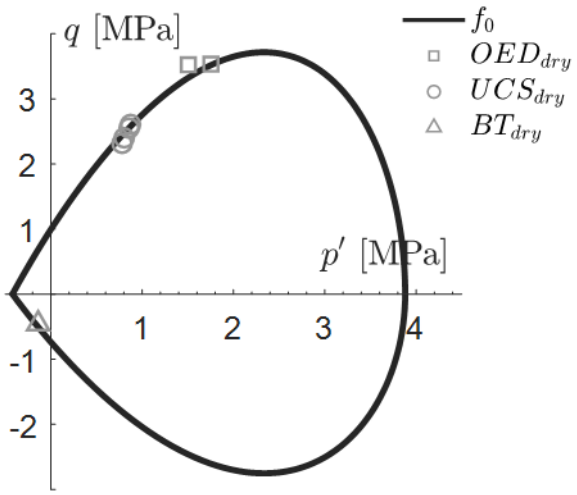

Figure 4. Yield surface for Gravina Calcarenite (Ciantia and Di Prisco 2016).

Table 2. The main physical and mechanical calcarenite rock parameters from Ciantia et al., (2015)

γ_{dry} $[kN/m^3]$	G_s [-]	e [-]	$\sigma_{c,dry}$ [MPa]	$\sigma_{t,dry}$ [MPa]	E_{dry} [MPa]	ν [-]
13.1	2.73	1.09	2.44	0.47	315	0.09

Following the installation procedure previously reported, the sleeve anchor bolt was installed in an intact calcarenite sample. To assess the effectiveness of the installation and its effect on the surrounding rock matrix, X-ray computed tomography (XCT) was herein employed, utilizing grayscale values as representative of the potential change of porosity and density of the rock material (Riccio et al., 2023). X-ray CT-scans were performed after drilling the hole and after the installation of the sleeve anchor bolt as shown in Figure 5.

The scans were optimised by adopting a beam energy of 200 kV and 40 W power. The images were acquired, reconstructed, and processed by using the multi-material surface determination VG STUDIO software.

The scans highlight the successful expansion of the anchor within the calcarenite, with a noteworthy gap around the anchor bolt, potentially affected by scan artefacts or minor rock disturbance effects (Figure 5b). Contrary to expectations, due to the soft rock involved, the X-ray CT scans do not reveal the formation of a plastic zone or significant rock damage at the anchor edge. This suggests that the installation was relatively non-disruptive to the rock mass but just locally in corresponding with the expanded sleeve fingers.

Figure 5c shows a preview scan after the pull-out test on calcarenite sample which indicates the propagation of a main fracture revealing the boundary effect on its propagation.

This direct experimental investigation of installation effects not only demonstrates the feasibility of the procedure but also provides insights into the pre-stressing effects on anchor bolts post-installation performance. The findings hence underscore the potential of small-scale X-ray CT for future studies aimed at optimizing anchor design.

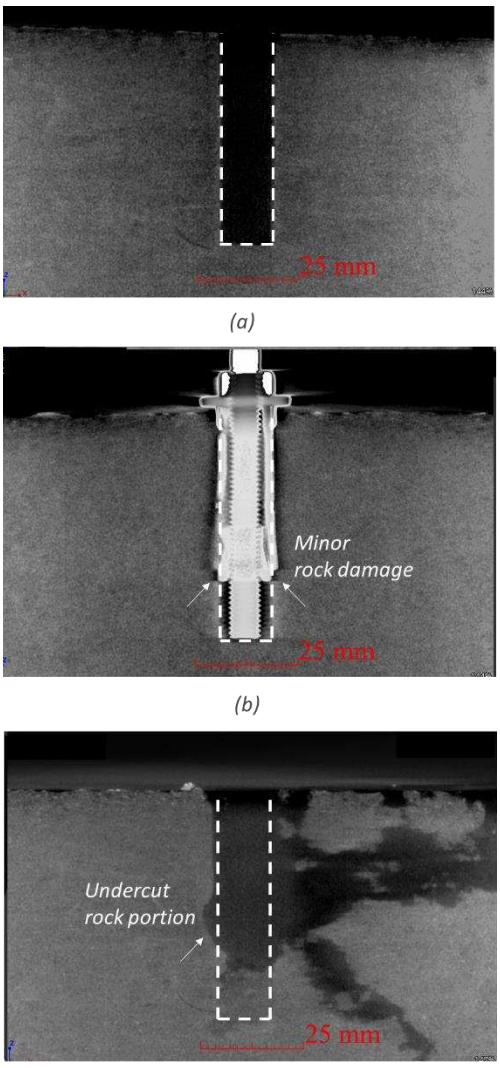

Figure 5. Cross sections of XTC-scans (a) after drilling the hole, (b) after the installation of the sleeve anchor bolt, and (c) after the preliminary pull-out test.

3 1G PHYSICAL TEST SET-UP

Figure 6 shows the 1g set-up for the small-scale physical test conducted on a calcarenite rock block. The goal was to evaluate the failure mechanism and the load capacity of the modelled RA under axial loading. Tests were performed up to large displacements highlighting the complex rock-anchor interaction problem.

The sleeve anchor bolt was installed following the methodology outlined in the previous section in a calcarenite block of $200 \times 150 \times 150\ mm$. Its rock properties are listed in Table 2. The load capacity of the anchor was preliminary estimated by means of current design analytical methods to identify a suitable load cell. To apply and transfer an axial load to the anchor bolt, an Instron UTM tensile tester was used, featuring a load cell with a maximum capacity of 50 kN and resolution of ±0.50%.

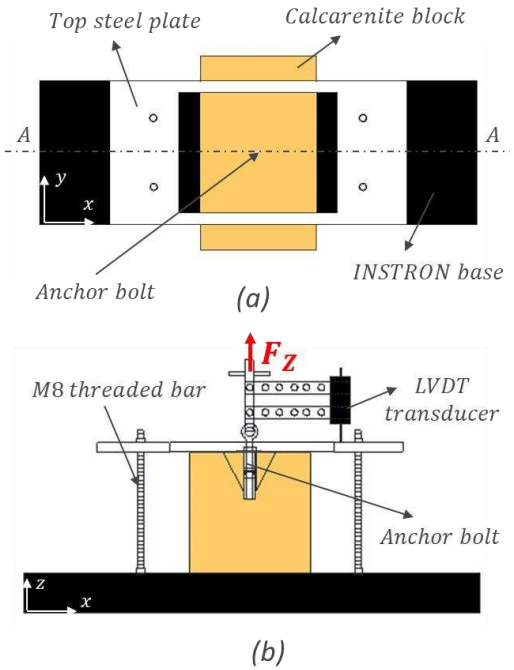

Figure 6. (a) Small-scale physical test set-up for the axial loading configuration with (b) cross section A-A at the centre of the calcarenite rock block.

The experimental apparatus included a connection between the load cell and the eye ring of the bolt via a steel slab, which also supported an LVDT transducer to measure displacement (Figure 6b).

The tensile load was applied with a constant rate of 0.05 mm/min facilitating the acquisition of accurate (displacement resolution 0.01 μm) load-displacement curves registered at control-displacement mode. The calcarenite block was securely constrained on the Instron base by using a top steel plate (Figure 6), designed to ensure the propagation of the full failure mechanism avoiding potential boundary effects. Specifically, the size of calcarenite block and the cut-out in the steel plate were estimated through preliminary analytical calculations of the cone failure expected following Kim and Cho, (2012).

The steel plate, equipped with four M8 holes for accommodating threaded bars, was screwed into the Instron base. The bars, secured with washers and nuts, held the rock block firmly in place.

4 TEST RESULTS

The model pullout test results were compared with the two analytical methods used in design practice: the ACI 349 (1985) and the Kim and Cho, (2012) approach. The ACI 349 (1985) method, derived using tests in concrete, calculates the axial capacity from the equilibrium of a rigid cone wedge with an inclination (θ_c) of 90° (45° inclined fractures from the anchor tip). In this method the tensile stress acting normally to the failure surface is considered in the equilibrium equation (Béton, 1994a). The tensile stress is empirically correlated to the compressive strength of the rock. The RA ultimate capacity is hence calculated as:

$$F_{ult} = \emptyset\, 0.33 \sqrt{\sigma_c}\, A_c \qquad (1)$$

where $\emptyset$ is an empirical strength reduction factor, σ_c is the uniaxial compressive strength of the rock, and A_c is the lateral surface of the cone of failure.

Based on field test observations, Kim and Cho, (2012) derived their model for grouted anchors, using a similar approach but using a cone failure inclinations of 90° for hard rocks and 60° for soft rocks (Brown, 2015). The pull-out capacity is determined by the expression:

$$F_{ult} = f_r + W_c \cos\theta_c \qquad (2)$$

and W_c is the weight of the cone wedge and f_r is the tensile strength on the failure surface expressed by:

$$f_r = \sigma_t \pi H^2 \tan(\theta_c/2)/\cos(\theta_c/2) \qquad (3)$$

where H is the height of the anchor and σ_t is the tensile strength of the rock,

Figure 7a illustrates the load-displacement curve from the pull-out test, alongside the predictions by the analytical methods. The test was conducted by executing a loading stage up to 5 mm (0.35D) (Point A), followed by an unloading stage to zero load (Point B). From this point a final stage leading to complete failure (Point C) was performed. Elastic behaviour was observed up to approximately 0.7 mm (0.05D), reaching the first peak and consequent crack formation. The maximum pull-out capacity recorded was 2.03 kN. The findings reveal that both analytical methods proposed underestimate the peak axial capacity upon the assumption on the full cone failure mode.

*Figure 7*b shows three snapshots taken during the test (Point A, C, and D). At Point A the crack of the failure wedge starts to appear at the surface.

After the unload phase, as axial displacements increase, a softening behaviour emerges, marked by the reduction in axial load up to the Point C, where the formation of a conical fracture on the surface appeared. Subsequent displacement led to the complete detachment of the rock cone, captured at Point D. The pullout test appeared to be characterised by localised failure mechanisms at the interface at the bottom of the anchor.

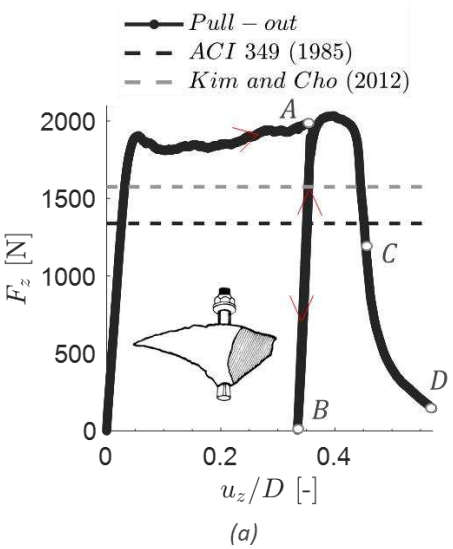

(a)

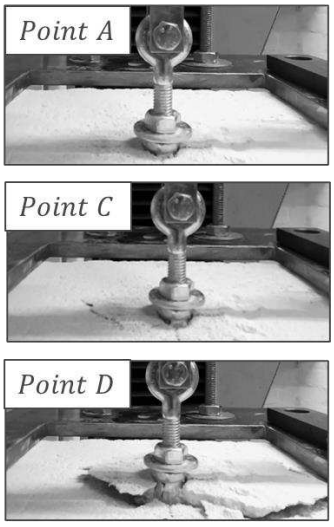

(b)

Figure 7. (a) Load-displacement curve for the axial loading test performed compared with the analytical methods presented and (b) images of the pull-out failure configurations at Point A, Point C, and Point D.

Once the displacements reach 6mm (0.42D), the failure transitions from a localised interface failure to a global cone shaped one. Whereas this transition emerges at lower displacement for the installation effect study. The geometrical distribution of the cone was not perfectly symmetric as shown in *Figure 7*b.

5 CONCLUSIONS

In this paper, a small-scale 1g physical testing framework was presented to evaluate the axial response of a sleeve anchor bolt, adopted as an analogue to model an innovative RA system, installed in calcarenite rock. Detailed insights into the anchor bolt installation procedure and its impact on calcarenite soft rock were provided by means of X-ray CT technology. Contrary to expectations, the scans did not reveal the presence of a plastic zone or fractures due to the installation procedure. The method provided appears promising at detecting potential rock damage and validating the robustness of the installation procedure. A pull-out test was conducted applying axial loading using an UTM Instron testing machine. The pull-out failure mode was observed and after large displacements this was followed by the noteworthy formation of an almost axisymmetric wedge. The comparison between the experimental load-displacement curve with analytical solutions highlight the underestimation of the axial capacity by using the analytical approach. These outcomes provide valuable insights for advancing RA design in ORE applications. The outcomes underscore the necessity for further investigation under varied loading and pre-tension conditions to enhance the current conservative design procedure.

ACKNOWLEDGEMENTS

This research is part of an industry funded studentship (ETP EIDP #182). Support of the industrial partner SCHOTTEL Marine Technologies and the Engineering Technology Partnership (ETP). The RSE Saltire International Collaboration Award "*Multiscale modelling of multidirectional cyclic behaviour of ORE anchoring systems*" (ID: 1938) is also gratefully acknowledged.

REFERENCES

Béton, C. E.-I. Du. (1994a). Fastenings To Concrete and Masonry Structures. Publishing, I C E, 104–110. https://doi.org/10.1680/ftcams.35423.0009

Béton, C. E.-I. Du. (1994b). Fastenings To Concrete and Masonry Structures. Publishing, I C E, c, 10–31. https://doi.org/10.1680/ftcams.35423.0003

Brown, E. T. (2015). Rock engineering design of post-tensioned anchors for dams - A review. Journal of Rock Mechanics and Geotechnical Engineering, 7(1), 1–13. https://doi.org/10.1016/j.jrmge.2014.08.001

Cerfontaine, B, Brown, M. J., Caton, A., Hunt, A., & Cresswell, N. (2021). Numerical modelling of rock anchor uplift capacity for offshore applications. September.

Cerfontaine, Benjamin, White, D., Kwa, K., Gourvenec, S., Knappett, J., & Brown, M. (2023). Anchor geotechnics for floating offshore wind : Current technologies and future innovations. Ocean Engineering, 279(August 2022), 114327. https://doi.org/10.1016/j.oceaneng.2023.114327

Ciantia, Matteo O., & Di Prisco, C. (2016). Extension of plasticity theory to debonding, grain dissolution, and chemical damage of calcarenites. International Journal for Numerical and Analytical Methods in Geomechanics, 40(3), 315–343. https://doi.org/10.1002/nag.2397

Ciantia, Matteo Oryem, Castellanza, R., & di Prisco, C. (2015). Experimental Study on the Water-Induced Weakening of Calcarenites. Rock Mechanics and Rock Engineering, 48(2), 441–461. https://doi.org/10.1007/s00603-014-0603-z

Cresswell, & Jeffcoate. (2016). Anchor Installation for the Taut Moored Tidal Platform PLAT-O. 3rd Asian Wave and Tidal Energy Conference, October 2016. https://s3-eu-west-1.amazonaws.com/assets-sustainablemarine-com/downloads/AWTEC-2016-Anchoring-Paper.pdf

IRENA-GWEC. (2022). SDG7 Energy Compact of the International Renewable Energy Agency (IRENA) and the Global Wind Energy Council (GWEC).

Kim, H. K., & Cho, N. J. (2012). A design method to incur ductile failure of rock anchors subjected to tensile loads. Electronic Journal of Geotechnical Engineering, 17 T, 2737–2746.

Lollino, P., & Andriani, G. F. (2017). Role of Brittle Behaviour of Soft Calcarenites Under Low Confinement: Laboratory Observations and Numerical Investigation. Rock Mechanics and Rock Engineering, 50(7), 1863–1882. https://doi.org/10.1007/s00603-017-1188-0

Randolph, M. F., Gaudin, C., Gourvenec, S. M., White, D. J., Boylan, N., & Cassidy, M. J. (2011). Recent advances in offshore geotechnics for deep water oil and gas developments. Ocean Engineering, 38(7), 818–834. https://doi.org/10.1016/j.oceaneng.2010.10.021

Riccio, T., Previtali, M., Ciantia, M. O., & Brown, M. J. (2023). P-y response in porous rock : numerical derivation with experimental validation. 9th International SUT OSIG Conference "Innovative Geotechnologies for Energy Transition," September 1357–1362. https://sut.org/event/osig2023/

Weerasinghe, R. B., & Littlejohn, G. S. (1997). Uplift capacity of shallow anchorages in weak mudstone. In Ground anchorages and anchored structures.

INTERNATIONAL SOCIETY FOR SOIL MECHANICS AND GEOTECHNICAL ENGINEERING

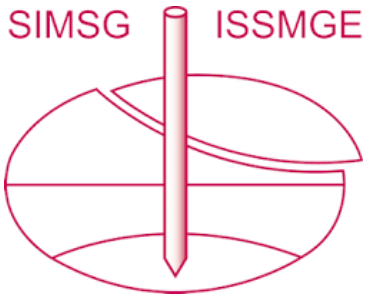

This paper was downloaded from the Online Library of the International Society for Soil Mechanics and Geotechnical Engineering (ISSMGE). The library is available here:

https://www.issmge.org/publications/online-library

This is an open-access database that archives thousands of papers published under the Auspices of the ISSMGE and maintained by the Innovation and Development Committee of ISSMGE.

The paper was published in the proceedings of the 5th European Conference on Physical Modelling in Geotechnics and was edited by Miguel Angel Cabrera. The conference was held from October 2nd to October 4th 2024 at Delft, the Netherlands.

To see the prologue of the proceedings visit the link below:

https://issmge.org/files/ECPMG2024-Prologue.pdf